

# Ferroelectric properties of lightly doped La:HfO<sub>2</sub> thin films grown by plasma-assisted atomic layer deposition

M. G. Kozodaev, A. G. Chernikova, E. V. Korostylev, M. H. Park, U. Schroeder, C. S. Hwang, and A. M. Markeev

Citation: [Appl. Phys. Lett.](#) **111**, 132903 (2017); doi: 10.1063/1.4999291

View online: <http://dx.doi.org/10.1063/1.4999291>

View Table of Contents: <http://aip.scitation.org/toc/apl/111/13>

Published by the [American Institute of Physics](#)

---

---



## SciLight

Sharp, quick summaries **illuminating**  
the latest physics research

Sign up for **FREE!**

**AIP**  
Publishing

# Ferroelectric properties of lightly doped La:HfO<sub>2</sub> thin films grown by plasma-assisted atomic layer deposition

M. G. Kozodaev,<sup>1</sup> A. G. Chernikova,<sup>1</sup> E. V. Korostylev,<sup>1</sup> M. H. Park,<sup>2</sup> U. Schroeder,<sup>2</sup> C. S. Hwang,<sup>3</sup> and A. M. Markeev<sup>1,a)</sup>

<sup>1</sup>Moscow Institute of Physics and Technology, Institutskii per. 9, 141700 Dolgoprudny, Moscow region, Russia

<sup>2</sup>NaMLab gGmbH/TU Dresden, Noethnitzer Strasse 64, 01187 Dresden, Germany

<sup>3</sup>Department of Materials Science and Engineering and Inter-University Semiconductor Research Center, Seoul National University, Seoul 08826, South Korea

(Received 7 August 2017; accepted 16 September 2017; published online 26 September 2017)

The structural and ferroelectric properties of lightly La-doped (1 mol. %) HfO<sub>2</sub> thin films grown by plasma-assisted atomic layer deposition were examined. An annealing temperature as low as 400 °C crystallized the film into the desired orthorhombic phase, which resulted in it displaying promising ferroelectric performance. The remanent polarization ( $P_r$ ) increased with annealing temperature, but the performance enhancement seemed to saturate at 500 °C. A slight decrease in the dielectric constant, which was associated with the preferential formation of a polar orthorhombic phase at higher temperatures, was also observed. The long-term wake-up effect, i.e., a marked rise in the  $2P_r$  value during field cycling, was demonstrated for films processed at all annealing temperatures. The presence of domain groups with opposite internal electric biases was found in the pristine state, while the internal bias distribution became more uniform during wake-up. The endurance of up to  $4 \times 10^8$  switching cycles without marked fatigue using bipolar pulses with a duration of 600 ns, and an amplitude of  $\pm 3$  MV/cm was demonstrated. *Published by AIP Publishing.*

<http://dx.doi.org/10.1063/1.4999291>

The recent discovery of ferroelectricity in doped hafnium oxide (HfO<sub>2</sub>)<sup>1</sup> demonstrated the possibility to overcome technical challenges facing conventional perovskite ferroelectrics.<sup>2</sup> Both ferroelectric HfO<sub>2</sub>-based layers and electrodes, typically TiN, can be grown by atomic layer deposition (ALD) with excellent conformality,<sup>3</sup> which means that they are fully compatible with complementary metal-oxide-semiconductor (CMOS) technology and allow the potential of three-dimensional structure formation.<sup>4</sup> However, the TiN/HfO<sub>2</sub> interface is usually imperfect and contains a high density of defects (e.g., oxygen vacancies). Because interfacial and bulk defects are considered as the root of several undesired effects such as wake-up, fatigue, imprint, and early breakdown, the use of inert electrodes could be required, as has proved effective in the case of perovskite materials.<sup>5</sup> In this regard, ALD can also be applied to Ir<sup>6</sup> or Ru<sup>7</sup> growth.

It has been suggested that the ferroelectricity in doped HfO<sub>2</sub> films is caused by the formation of the polar orthorhombic phase (o-phase, space group Pca2<sub>1</sub>) under certain conditions.<sup>8,9</sup> Incorporation of dopants with a large atomic radius (e.g., Y, La, and Gd) into HfO<sub>2</sub> has been proven experimentally to be one of the most effective methods to promote the formation of the o-phase<sup>10–13</sup> and consequently provide promising ferroelectric responses. In particular, the combination of a relatively high double remanent polarization ( $2P_r$ ) value ( $\sim 33 \mu\text{C}/\text{cm}^2$ ) and endurance following  $10^8$  switching cycles without any fatigue (decrease in the  $2P_r$  value with cycling) was recently demonstrated for La-doped HfO<sub>2</sub> (La:HfO<sub>2</sub>).<sup>11</sup> Unfortunately, La:HfO<sub>2</sub> films possess a higher crystallization temperature than that of pure HfO<sub>2</sub> for

the same thickness (or grain size), which might be because La is an amorphization dopant in HfO<sub>2</sub>.<sup>14</sup> As a result, the use of La:HfO<sub>2</sub> thin films in a standard back-end-of-line (BEOL) process for ferroelectric random access memory is quite challenging compared to that of other doped HfO<sub>2</sub> or Hf<sub>x</sub>Zr<sub>1–x</sub>O<sub>2</sub> ferroelectrics, which possess crystallization temperatures as low as 400–450 °C over a wide thickness range down to 2.5 nm.<sup>15–19</sup> Indeed, even a relatively low level of La doping (2.1 at. %) resulted in 10-nm-thick La:HfO<sub>2</sub> films retaining their amorphous state after annealing at temperatures below 550 °C. These results indicate that a lower La doping level may result in a lower crystallization temperature, as predicted by the literature.<sup>20</sup> Therefore, this work explores the possibility of lowering the crystallization temperature of La:HfO<sub>2</sub> to a BEOL-compatible level (400 °C) by decreasing its La content while maintaining the preferential formation of the o-phase.

It has been shown that the dielectric layer should be kept in an amorphous state before rapid thermal annealing (RTA) to induce crystallization or during top electrode deposition to avoid undesirable preliminary crystallization and consequently achieve a high remanent polarization ( $P_r$ ).<sup>21,22</sup> However, conventional ALD or chemical vapor deposition processes for TiN top electrode fabrication require a rather high deposition temperature (400–450 °C),<sup>23</sup> which may induce the crystallization of even ultrathin HfO<sub>2</sub>-based films.<sup>16</sup> Plasma-assisted atomic layer deposition (PAALD) allows the deposition temperature to be lowered to  $\sim 300$  °C<sup>4,24</sup> and, therefore, can be applied for this task.

We utilized PAALD to prepare a set of 10-nm-thick La:HfO<sub>2</sub> films with a low La concentration (1 mol. %) in order to investigate their ferroelectric and structural properties

<sup>a)</sup>Electronic mail: [markeev.am@mipt.ru](mailto:markeev.am@mipt.ru)

after rapid thermal annealing (RTA) at 400–500 °C. The structural properties of the annealed La:HfO<sub>2</sub> films were examined by grazing-incidence X-ray diffraction (GIXRD). The ferroelectric properties of annealed complete MFM structures were investigated by the positive-up–negative-down (PUND) technique. The detailed description of sample preparation and experimental techniques is presented in the [supplementary material](#).

First, the crystalline structure of La:HfO<sub>2</sub> films annealed at different temperatures was investigated [Fig. 1(a)]. All films, including those annealed at 400 °C, were polycrystalline with clear diffraction peaks, which were attributed to the o-phase and/or tetragonal phase (t-phase, space group P4<sub>2</sub>/nmc).

The diffraction peak located at  $\approx 30.4^\circ$  could consist of [111]<sub>o</sub> and [111]<sub>t</sub> peaks, while more precise identification is quite challenging due to the structural identity of mentioned phases. The presence of the cubic phase (c-phase, space group Fm3m) could also not be completely excluded, but according to the literature data, it becomes stable only at a high La concentration.<sup>14,26</sup> It is worth noting that the peak near  $\sim 30.4^\circ$  shifted monotonically to lower the  $2\theta$  value with increasing RTA temperature, whereas that near  $35.5^\circ$  shifted to a higher  $2\theta$  value [Fig. 1(b)] under identical RTA conditions, which indicates the variation of the lattice parameters of the films with changing RTA temperature. The extracted lattice parameters from these peak positions are presented in Fig. 1(c). Here, the lattice parameter “c” refers to the longest axis (a for the o-phase and c for the t-phase), while “a” refers to the two shorter axes (b and c for the o-phase and a for the t-phase). The aspect ratio (c/a for the t-phase and  $2a/(b+c)$  for the o-phase) increases from 1.023 to 1.028 with rising annealing temperature from 400 to 500 °C, which is similar to those one observed for Si-, Al-, and Gd-doped HfO<sub>2</sub> thin films with strong ferroelectricity.<sup>27</sup> Therefore, the

La:HfO<sub>2</sub> film could be ferroelectric after RTA at just 400 °C according to the presented structural analysis. At the same time, an increase in the relative fraction of the o-phase with rising annealing temperature can be expected because of the corresponding increase in the aspect ratio of the unit cell.

The presence of a small amount of the monoclinic phase (m-phase) was also identified for the films crystallized all RTA temperatures because weak peaks located at  $\sim 28.5^\circ$  and  $\sim 31.6^\circ$ , attributed to  $[-111]_m$  and  $[111]_m$  reflections, respectively, were found in all GIXRD patterns presented in Fig. 1(a). The precise calculation of the m-phase fraction is quite difficult given the proximity of the peak positions from different phases and rather broad diffraction peaks. Therefore, only the relative ratio ( $R_m$ ) of the integrated area of the peaks, corresponding to the m-phase, to the sum of all peak intensities in the  $2\theta$  region  $27\text{--}33^\circ$ , is presented, which might be sufficient to justify the following analysis. The  $R_m$  value is  $\sim 20\%$  for the film annealed at 400 °C and decreases slightly to  $\sim 15\%$  for films annealed at 450 and 500 °C. However, the  $R_m$  increase is expected at higher annealing temperature because of the possible increased grain size, which decreases the surface energy contribution. The surface/grain boundary/interface energy is the critical factor affecting the stabilization of the o-phase.<sup>8,27</sup> To get insights into this seemingly contradictory result, scanning electron microscopy (SEM) was used to examine the grain size distribution in the samples. The estimated median grain radius is 9.4 nm, and it is almost constant for films annealed at different temperatures (the related SEM images are presented in the [supplementary material](#)), which could be related to the rather narrow range of RTA temperatures used here and the strong ability of La to suppress grain growth.<sup>28</sup> It is speculated that the slight decrease in  $R_m$  observed in Fig. 1(a) arises from the presence of remaining amorphous regions (e.g., near the ferroelectric/electrode interfaces) after RTA

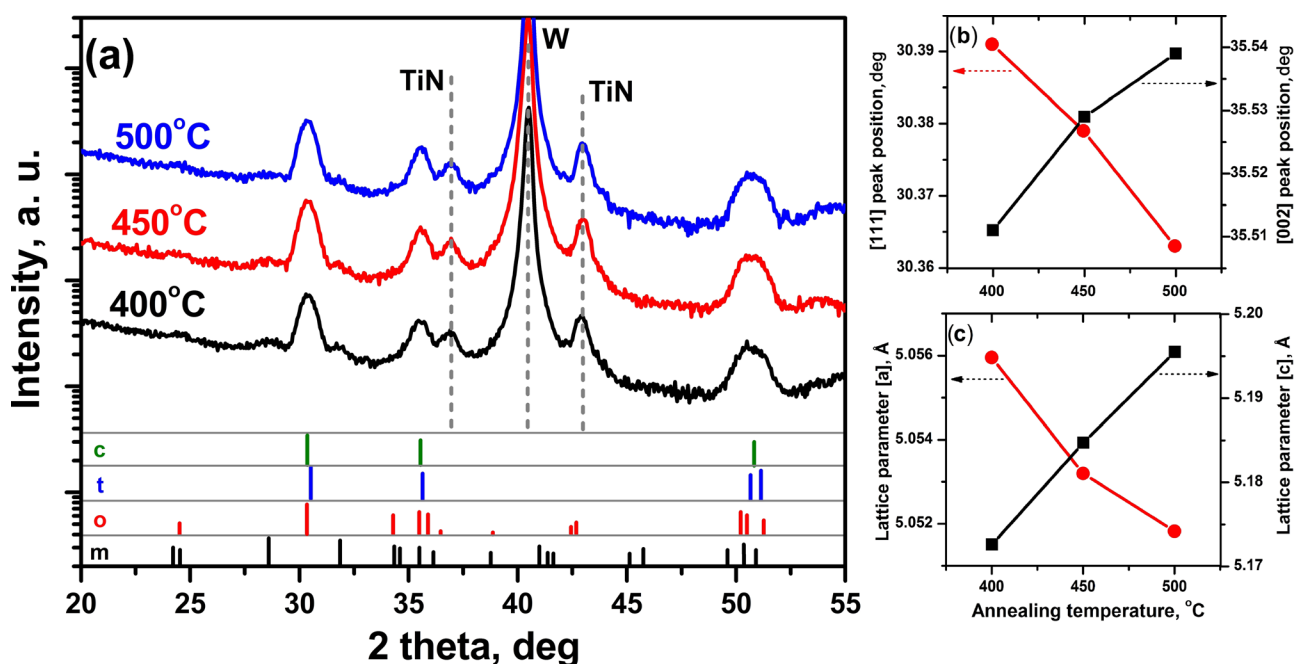


FIG. 1. (a) GIXRD spectra, collected from La:HfO<sub>2</sub> films, annealed at 400, 450, and 500 °C with calculated powder diffraction patterns;<sup>8,25</sup> (b) [111] and [002] peak positions as a function of annealing temperature; (c) variations in the lattice parameters as a function of annealing temperature.

at 400 °C. The remaining amorphous material will crystallize into the o-phase (or partially into the t-phase) by heterogeneous nucleation at the amorphous/o-phase interface during RTA at 450 or 500 °C because the major crystalline phase after RTA at 400 °C is the o-phase.

The ferroelectric response of the films was analyzed. Dynamic switching current-electric field (I-E) measurements of film, annealed at 400 °C, in the pristine (i.e., before field cycling) state showed current peaks both at negative and positive voltages, which is typical for ferroelectric materials [Fig. 2(a)]. However, multiple current peaks in response to the first voltage sweep on the pristine structure were observed both at positive and negative voltages, which is clearly attributed to the switching non-uniformity of the ferroelectric film and is caused by the presence of groups of domains with different internal (built-in) biases.<sup>29</sup> The voltage sweep schemes used for their distinction are presented in Figs. 2(c) and 2(e), while the related current responses are presented in Figs. 2(d) and 2(f). The repeated application of triangular sweeps with the same amplitude and direction of the electric field provided test results compatible with those from the PUND tests. According to Figs. 3(c) and 3(d), after the first ND-PU cycle with an amplitude of  $\pm 3$  MV/cm, all switchable ferroelectric domains in the film become polarized to the “positive” direction. After that, by applying a ND

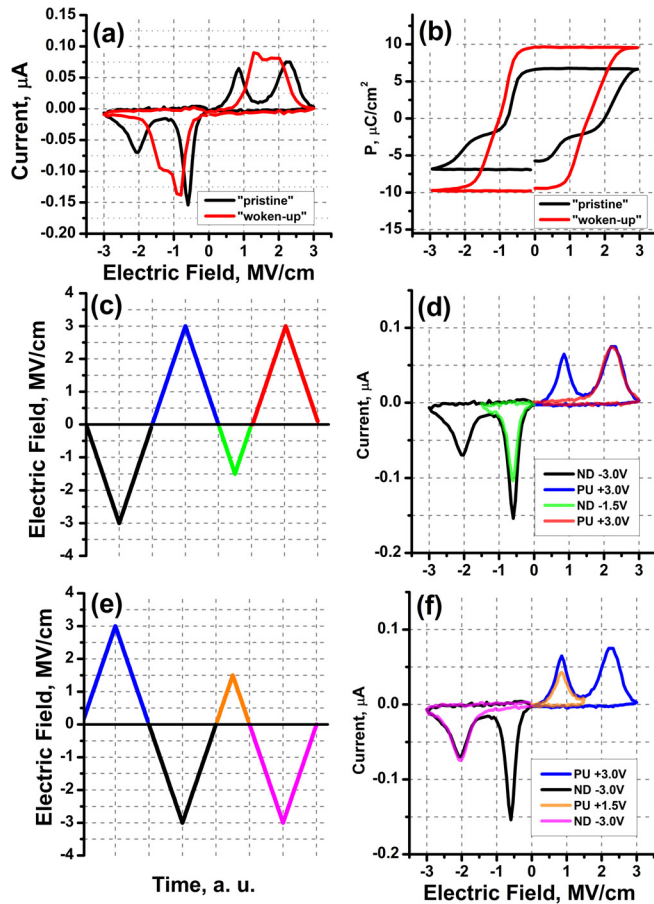


FIG. 2. (a) I-E characteristics of the La:HfO<sub>2</sub> film, annealed at 400 °C, in “pristine” (black) and “woken-up” ( $10^5$  switching cycles at  $\pm 3$  MV/cm) states (red) with the corresponding P-E loops (b). (c) and (e) P-U-N-D measurement voltage sweep and (d) and (f) corresponding I-E characteristics of the same film (the colors of the voltage sweep curves correspond to related current responses).

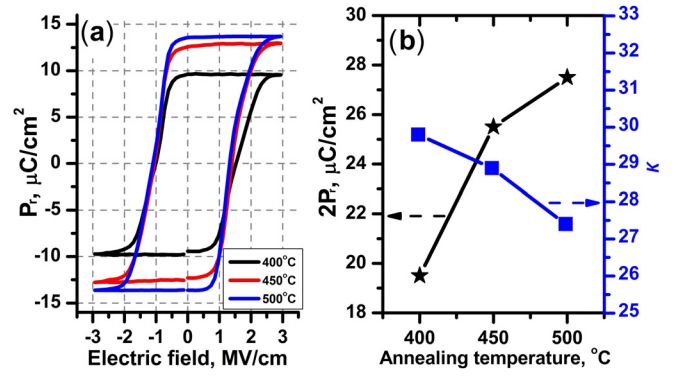


FIG. 3. (a) P-E hysteresis loops, measured from La:HfO<sub>2</sub> films, annealed at 400, 450, and 500 °C, after  $10^5$  switching cycles at  $\pm 3$  MV/cm. (b)  $2P_r$  and  $k$  value as a function of RTA temperature.

voltage sweep with a smaller amplitude of  $-1.5$  MV/cm, only one group of the domains (with a lower relative switching field  $E_s$  of  $\sim -0.56$  MV/cm) switches to the “negative” direction. The subsequent PU sweep with an amplitude of  $+3$  MV/cm revealed the back-switching field  $E_{bs}$  of this group of domains, which was relatively high ( $E_{bs} \sim +2.36$  MV/cm). A schematic picture, illustrating the described procedure, is presented in the supporting material. The peak at  $+0.84$  MV/cm, which can be clearly observed after the first ND-PU cycle with an amplitude of  $\pm 3$  MV/cm, disappeared after the last procedure. It becomes obvious that this peak originates from the switching of domains belonging to another group. Therefore, the first group of domains has a hysteresis curve that is shifted toward the positive direction along the electric field axis. This shift can be presented as a function of the internal bias field  $E_{bias}$ , while the average coercive field  $E_c$  of these domains can also be roughly evaluated from  $E_s$  and  $E_{bs}$  peak positions.

The following equations were used to estimate  $E_{bias}$  and  $E_c$ :

$$E_c = \left| \frac{E_s - E_{bs}}{2} \right|, \quad (1)$$

$$E_{bias} = \frac{E_s + E_{bs}}{2}. \quad (2)$$

According to these equations, the  $E_{bias}$  of  $\sim 0.90$  MV/cm and the  $E_c$  of  $\sim 1.45$  MV/cm were calculated for the first group of domains from the dynamic current curve presented in Fig. 2(d). A similar procedure was used to reveal the  $E_{bias}$  and  $E_c$  of the second group of domains [Figs. 2(e) and 2(f)]; the  $E_{bias}$  of  $\sim -0.55$  MV/cm and  $E_c$  of  $\sim 1.40$  MV/cm were found for this case.

The presence of two types of ferroelectric domains with almost equal  $E_c$  and different  $E_{bias}$  in the pristine state, which was also observed earlier for hard Pb(Ti, Zr)O<sub>3</sub> ceramics,<sup>30</sup> may be caused by interfacial defects (possibly oxygen vacancies) near both top and bottom film interfaces. The generation of oxygen vacancies could be caused by oxygen migration to the TiN layers, and they can diffuse to the domain wall regions and pin the domains.<sup>30</sup> Multiple switches could result in a more uniform defect distribution across the ferroelectric layer and a change in their occupancy, which was earlier observed during the wake-up process for other HfO<sub>2</sub>-based



ferroelectrics.<sup>31–33</sup> A similar behavior was also observed here: after the wake-up cycling (i.e., after  $10^5$  switches by pulses with a duration of 600 ns and an amplitude of 3 MV/cm), the multiple current peaks moved toward each other [Fig. 2(a)]. However, even after this procedure, the resulting current response contained multiple components, which indicates that only partial internal bias relaxation occurred. Almost full relaxation of the internal bias occurred for the second group of domains, while the internal bias decreased to  $\sim 0.5$  MV/cm for the first. The same procedure was performed for the films annealed at higher temperatures with a similar qualitative result. The extracted coercive fields and biases for the pristine and woken-up states are presented in the [supplementary material](#).

The  $2P_r$  value, which was extracted from  $P_r$ -E hysteresis curves [Fig. 2(b)], increased markedly following the wake-up process from  $\sim 12$  to  $\sim 20 \mu\text{C}/\text{cm}^2$ . Besides the partial relaxation of the built-in bias during wake-up, the previously inactive (or pinned) domains in the pristine state (presumably related to defects) became involved in the switching process after the wake-up process. The transformation from the t- to o-phase near the ferroelectric/electrode interface, as shown previously for other  $\text{HfO}_2$ -based ferroelectrics, could be among the reasons for such behavior.<sup>31,32</sup>

The improvement of the ferroelectric properties of the films with increasing annealing temperature was subsequently examined. The  $P_r$ -E hysteresis loops for films after RTA at 400, 450, or 500 °C and  $10^5$  wake-up cycles are presented in Fig. 3(a).

The  $2P_r$  value increases from  $\sim 20$  to  $\sim 25 \mu\text{C}/\text{cm}^2$  with rising RTA temperature from 400 to 450 °C. A further increase in the RTA temperature caused a minor  $2P_r$  rise of only  $\sim 7\%$ , indicating a tendency to saturation. According to the structural analysis presented above, the observed initial increase in the  $2P_r$  value can be attributed to increased crystallization of the film into the o-phase. The formation of the o-phase was further confirmed by the analysis of the small-signal C-V curves measured after  $10^5$  switches. Figure 3(b) shows the variation of the extracted  $k$  values along with the  $2P_r$  values with increasing RTA temperature. Here, the  $k$ -values were taken at an electric field strength of  $+3$  MV/cm, i.e., outside the switching regions, to represent only the linear dielectric contribution. “The  $k$  value decreased monotonically from  $\sim 30.0$  to  $\sim 27.5$  with increasing RTA temperature from 400 to 500 °C. According to the literature data, the o-phase is characterized by a  $k$ -value of  $\approx 30$ , while the one for the t-phase is  $\approx 35$ . For the m-phase, it is in the range of  $\approx 15$ – $20$ , which is close to that of the amorphous  $\text{HfO}_2$ . All these phases can be present in the  $\text{La}:\text{HfO}_2$  films, and their relative portion can change with the RTP temperature increase. The GIXRD showed a slight decrease in the m-phase relative ratio ( $R_m$ ) with the increasing RTP temperature, which could have increased the  $k$  value. However, the observed considerable increase in  $P_r$  with the RTP temperature indicates the effective transition of the t-phase to the o-phase, which is consistent with the  $k$  value decrease in the overall film. This means that the t- to o-phase transition has a more pronounced role in the  $k$  evolution compared to the decrease in amorphous and m-phase portion with the increasing RTP temperature.”

Finally, the endurance characteristics of the  $\text{La}:\text{HfO}_2$  films were examined. The change in  $2P_r$  with the increasing number of switching cycles is presented in Fig. 4. A marked wake-up effect is observed up to almost  $10^6$  switching cycles irrespective of the RTA temperature. After such prolonged wake-up, slight fatigue (decrease in  $2P_r$  by  $\sim 10\%$ ) was detected. Overall, the endurance performance of the samples was rather limited. The film annealed at 400 °C could be cycled up to  $4 \times 10^8$  times, but then a hard breakdown occurred. A slight endurance decrease (down to  $\sim 2 \times 10^8$ ) was also observed with increasing RTA temperature. It is worth noting that lowering the switching pulse amplitude to 2.5 MV/cm resulted in a significant endurance improvement up to  $1 \times 10^{10}$  cycles with no hard breakdown (Fig. 4). However, the lower switching field resulted in a lower maximum  $2P_r$  value ( $\sim 13 \mu\text{C}/\text{cm}^2$  at 500 °C). Also, the samples showed noticeable fatigue (decrease in  $2P_r$  by  $\sim 60\%$ ) after  $\sim 10^7$  switching cycles. It is believed that such limited endurance might be caused by imperfect interfacial layers between the ferroelectric and electrodes because oxygen vacancies are known to facilitate breakdown mechanisms in  $\text{HfO}_2$ .<sup>33</sup> Therefore, inert electrode utilization may overcome this problem.

In conclusion, feasible ferroelectric performance was achieved by PAALD-grown  $\text{La}:\text{HfO}_2$  films with a La concentration of 1 mol. % even when RTA was performed at just 400 °C, which is compatible with standard BEOL processes. The obtained  $2P_r$  value was  $\sim 20 \mu\text{C}/\text{cm}^2$ , and the film could endure up to  $4 \times 10^8$  switching cycles under applied bipolar pulses of  $\pm 3$  MV/cm and 600 ns. Interestingly, increasing the RTA temperature up to 500 °C slightly decreased the undesirable m-phase content by transformation into the ferroelectric o-phase. As a result, the  $2P_r$  value of the film was increased to  $\sim 27 \mu\text{C}/\text{cm}^2$ . The current results may be compared with those of a previous study of  $\text{La}:\text{HfO}_2$  films with a slightly higher La concentration.<sup>11</sup> The decrease in the La content resulted in a sizable annealing temperature decrease from  $\sim 550$  to 400 °C while keeping a rather high  $2P_r$  value. Moreover, promising endurance characteristics were also achieved. Furthermore, because of its low crystallization temperature, 1 mol. %  $\text{La}:\text{HfO}_2$  competes with the well-studied  $\text{Hf}_{0.5}\text{Zr}_{0.5}\text{O}_2$ , which can be processed at a similar RTA temperature. However,  $\text{Hf}_{0.5}\text{Zr}_{0.5}\text{O}_2$  films demonstrated the marked fatigue (decrease in  $2P_r$  by  $\sim 20\%$  after  $1 \times 10^8$  switching cycles)<sup>34</sup> compared with that for the  $\text{La}:\text{HfO}_2$  films in this work. Nonetheless, methods to further improve the endurance characteristics of

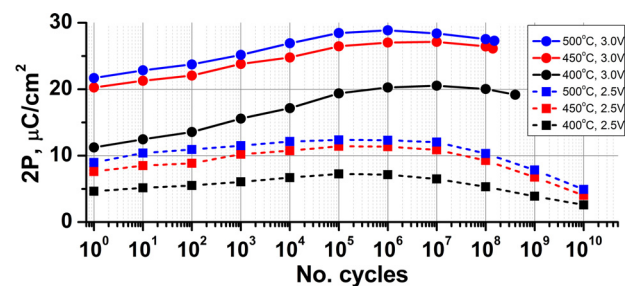


FIG. 4. Endurance characteristics of  $\text{La}:\text{HfO}_2$  films, annealed at 400, 450, and 500 °C ( $\pm 3.0/2.5$  MV/cm, 600 ns). A hard breakdown occurred after the maximum switching cycles for an applied switching field of 3 MV/cm (circle symbols), which was not the case for 2.5 MV/cm (square symbols).

such films are still highly desired to make the material compatible with the requirements for a universal memory.

See [supplementary material](#) for the details of sample preparation, measurement techniques, grain size analysis (SEM images), and the information related to the internal biases calculation.

The ALD growth of La:HfO<sub>2</sub> films and their structural and electrical properties investigations were supported by Russian Science Foundation (Project. No 14-19-01645-P) with the equipment of MIPT Shared Facilities Center supported by the Ministry of Education and Science of Russian Federation (Grant No. RFMEFI59417X0014).

M.H.P. acknowledges the support by a Humboldt postdoctoral fellowship from the Alexander von Humboldt Foundation for studies on the grain sizes distribution.

C.S.H. acknowledges the support by the Global Research Laboratory Program (2012K1A1A2040157) of the National Research Foundation of Korea (NRF) for calculations of La:HfO<sub>2</sub> lattice parameters.

- <sup>1</sup>T. S. Boescke, J. Mueller, D. Brauhaus, U. Schroeder, and U. Boettger, *Appl. Phys. Lett.* **99**, 102903 (2011).
- <sup>2</sup>T. Mikolajick, C. Dehm, W. Hartner, I. Kasko, M. Kastner, N. Nagel, M. Moert, and C. Mazure, *Microelectron. Reliab.* **41**, 947 (2001).
- <sup>3</sup>I. J. M. Erkens, M. A. Verheijen, H. C. M. Knoop, W. Keuning, F. Roozeboom, and W. M. M. Kessels, *J. Chem. Phys.* **146**, 052818 (2017).
- <sup>4</sup>M. G. Kozodaev, Y. Y. Lebedinskii, A. G. Chernikova, S. N. Polyakov, and A. M. Markeev, *Phys. Status Solidi A* **214**(6), 1700056 (2017).
- <sup>5</sup>C.-K. Huang, Y.-K. Chiou, Y.-C. Chu, T.-B. Wu, and C.-J. Tsai, *J. Electrochem. Soc.* **153**(6), F115–F119 (2006).
- <sup>6</sup>M. Mattinen, J. Hamalainen, M. Vehkamäki, M. J. Heikkilä, K. Mizohata, P. Jalkanen, J. Raisanen, M. Ritala, and M. Leskela, *J. Phys. Chem. C* **120**, 15235 (2016).
- <sup>7</sup>K. V. Egorov, Y. Y. Lebedinskii, A. A. Soloviev, A. A. Chouprik, A. Y. Azarov, and A. M. Markeev, *Appl. Surf. Sci.* **419**, 107 (2017).
- <sup>8</sup>R. Materlik, C. Kuenneth, and A. Kersch, *J. Appl. Phys.* **117**, 134109 (2015).
- <sup>9</sup>X. Sang, E. D. Grimley, T. Schenk, U. Schroeder, and J. M. LeBeau, *Appl. Phys. Lett.* **106**, 162905 (2015).
- <sup>10</sup>J. Mueller, U. Schroeder, T. S. Boescke, I. Mueller, and U. Boettger, *J. Appl. Phys.* **110**, 114113 (2011).
- <sup>11</sup>A. G. Chernikova, D. S. Kuzmichev, D. V. Negrov, M. G. Kozodaev, S. N. Polyakov, and A. M. Markeev, *Appl. Phys. Lett.* **108**, 242905 (2016).
- <sup>12</sup>M. Hoffmann, U. Schroeder, T. Schenk, T. Shimizu, H. Funakubo, O. Sakata, D. Pohl, M. Drescher, C. Adelman, R. Materlik, A. Kersch, and T. Mikolajick, *J. Appl. Phys.* **118**, 072006 (2015).
- <sup>13</sup>R. Batra, T. D. Huan, G. A. Rossetti, Jr., and R. Ramprasad, “Dopants promoting ferroelectricity in Hafnia: Insights from A comprehensive chemical space exploration,” preprint [arXiv:1707.04211v1](#) [cond-mat.mtrl-sci] (2017).
- <sup>14</sup>S. V. Ushakov, C. E. Brown, and A. Navrotsky, *J. Mater. Res.* **19**, 693–696 (2004).
- <sup>15</sup>M. H. Park, H. J. Kim, Y. J. Kim, W. Lee, T. Moon, and C. S. Hwang, *Appl. Phys. Lett.* **102**, 242905 (2013).
- <sup>16</sup>A. Chernikova, M. Kozodaev, A. Markeev, D. Negrov, M. Spiridonov, S. Zarubin, O. Bak, P. Buragohain, H. Lu, E. Suvorova, A. Gruverman, and A. Zenkevich, *ACS Appl. Mater. Interfaces* **8**, 7232 (2016).
- <sup>17</sup>A. Chouprik, A. Chernikova, A. Markeev, V. Mikheev, D. Negrov, M. Spiridonov, S. Zarubin, and A. Zenkevich, *Microelectron. Eng.* **178**, 250–253 (2017).
- <sup>18</sup>O. M. Orlov, A. M. Markeev, A. V. Zenkevich, A. G. Chernikova, M. V. Spiridonov, R. A. Izmaylov, and E. S. Gornev, *Russ. Microelectron.* **45**(4), 262–269 (2016).
- <sup>19</sup>D. R. Islamov, A. G. Chernikova, M. G. Kozodaev, A. M. Markeev, T. V. Perevalov, V. A. Gritsenko, and O. M. Orlov, *JETP Lett.* **102**(8), 544–547 (2015).
- <sup>20</sup>A. Navrotsky, *J. Mater. Chem.* **15**, 1883 (2005).
- <sup>21</sup>A. Chernikova, M. Kozodaev, A. Markeev, Y. Matveev, D. Negrov, and O. Orlov, *Microelectron. Eng.* **147**, 15 (2015).
- <sup>22</sup>M. H. Park, Y. H. Lee, H. J. Kim, Y. J. Kim, T. Moon, K. D. Kim, J. Mueller, A. Kersch, U. Schroeder, T. Mikolajick, and C. S. Hwang, *Adv. Mater.* **27**, 1811 (2015).
- <sup>23</sup>C. H. Ahn, S. G. Cho, H. J. Lee, K. H. Park, and S. H. Jeong, *Met. Mater. Int.* **7**(6), 621 (2001).
- <sup>24</sup>S. B. S. Heil, E. Langereis, F. Roozeboom, M. C. M. van de Sanden, and W. M. M. Kessels, *J. Electrochem. Soc.* **153**(11), G956–G965 (2006).
- <sup>25</sup>The International Center for Diffraction Data (ICDD). PDF Card No. 00-034-0104.
- <sup>26</sup>V. V. Kaichev, T. P. Smirnova, L. V. Yakovkina, E. V. Ivanova, M. V. Zamoryanskaya, A. A. Saraev, V. A. Pustovarov, T. V. Perevalov, and V. A. Gritsenko, *Mater. Chem. Phys.* **175**, 200–205 (2016).
- <sup>27</sup>M. H. Park, T. Schenk, C. M. Fancher, E. D. Grimley, C. Zhou, C. Richter, J. M. LeBeau, J. L. Jones, T. Mikolajick, and U. Schroeder, *J. Mater. Chem. C* **5**, 4677 (2017).
- <sup>28</sup>G. R. Waetzig, S. W. Depner, H. Asayesh-Ardakani, N. D. Cultrara, R. Shahbazian-Yassar, and S. Banerjee, *Chem. Sci.* **7**, 4930 (2016).
- <sup>29</sup>T. Schenk, M. Hoffmann, J. Ocker, M. Pesic, T. Mikolajick, and U. Schroeder, *ACS Appl. Mater. Interfaces* **7**, 20224 (2015).
- <sup>30</sup>K. Carl and K. H. Hardtl, *Ferroelectrics* **17**, 473–486 (1977).
- <sup>31</sup>M. Pesic, F. P. G. Fengler, L. Larcher, A. Padovani, T. Schenk, E. D. Grimley, X. Sang, J. M. LeBeau, S. Slesazeck, U. Schroeder, and T. Mikolajick, *Adv. Funct. Mater.* **26**, 4601 (2016).
- <sup>32</sup>E. D. Grimley, T. Schenk, X. Sang, M. Pesic, U. Schroeder, T. Mikolajick, and J. M. LeBeau, *Adv. Electron. Mater.* **2**, 1600173 (2016).
- <sup>33</sup>D. Zhou, J. Xu, Q. Li, Y. Guan, F. Cao, X. Dong, J. Mueller, T. Schenk, and U. Schroeder, *Appl. Phys. Lett.* **103**, 192904 (2013).
- <sup>34</sup>S. Zarubin, E. Suvorova, M. Spiridonov, D. Negrov, A. Chernikova, A. Markeev, and A. Zenkevich, *Appl. Phys. Lett.* **109**, 192903 (2016).